

Kondo effect and superconductivity in $\text{Nd}_{2-x}\text{Ce}_x\text{CuO}_{4-\delta}$ compounds

J. L. Peng and R. N. Shelton

Department of Physics, University of California-Davis, Davis, California 95616

H. B. Radousky

Lawrence Livermore National Laboratory, P.O. Box 808, Livermore, California 94550

(Received 24 July 1989)

Samples of $\text{Nd}_{2-x}\text{Ce}_x\text{CuO}_{4-\delta}$ ($0 \leq x \leq 0.2$) were prepared by annealing both in air and under vacuum (10^{-5} Torr). Powder x-ray-diffraction patterns indicated that all samples consisted of a single-phase Nd_2CuO_4 -type tetragonal structure with crystal symmetry $I4/mmm$. Electrical resistivity measurements showed that all Ce-doped $\text{Nd}_2\text{CuO}_{4-\delta}$ samples annealed in air and those annealed in vacuum with $x < 0.17$ demonstrate a resistivity minimum (Kondo effect) resulting from the combination of magnetic and phonon scattering. Magnetic susceptibility and electrical resistivity measurements reflect the influence of crystal-field effects below 55 K. The linear temperature-dependent term of the resistivity typical of metallic behavior in the high- T_c oxides exists across the whole range of Ce concentration, with the exception of the host compound $\text{Nd}_2\text{CuO}_{4-\delta}$, which is an insulator. This indicates that a model of metal-insulator transition is not appropriate in describing the occurrence of superconductivity in $\text{Nd}_{2-x}\text{Ce}_x\text{CuO}_{4-\delta}$.

INTRODUCTION

The discovery of superconductivity in the $R_2\text{CuO}_{4-\delta}$ system ($R = \text{Pr}$, Nd , and Sm) (Ref. 1) by a combination of Ce doping and oxygen reduction has generated a great deal of interest. Immediately following this discovery, superconductivity in $\text{Nd}_{2-x}\text{Th}_x\text{CuO}_{4-\delta}$, $\text{Pr}_{2-x}\text{Th}_x\text{CuO}_{4-\delta}$, and $\text{Eu}_{2-x}\text{Ce}_x\text{CuO}_{4-\delta}$ was observed.^{2,3} All of these superconductors have the same Nd_2CuO_4 -type structure,^{4,5} with oxygen deficiency achieved by annealing in a reducing atmosphere. The preparation of single-phase materials for these compounds is a delicate process in comparison with the other high- T_c copper oxides. Hall measurements^{1,6,7} indicate that these materials belong to the family of layered copper oxide superconductors where electrons are the charge carriers above T_c . This behavior contrasts sharply with that of the previously known high- T_c cuprates, which involve holes as the carriers responsible for the conductivity. Although the Nd_2CuO_4 -type structure is closely related to that of the La_2CuO_4 compound, a significant structural difference between the La_2CuO_4 and $R_2\text{CuO}_4$ compounds is that the Cu atoms are octahedrally coordinated by oxygens in La_2CuO_4 , but in the $R_2\text{CuO}_4$ materials, the coordination is square planar. In this paper, the results on the preparation, x-ray diffraction, magnetization characterization, and dc resistivity measurements of $\text{Nd}_{2-x}\text{Ce}_x\text{CuO}_{4-\delta}$ are reported. The dc resistivity measurements show evidence for the occurrence of a Kondo effect in the $\text{Nd}_{2-x}\text{Ce}_x\text{CuO}_{4-\delta}$ compounds.

EXPERIMENTAL DETAILS

Samples of $\text{Nd}_{2-x}\text{Ce}_x\text{CuO}_{4-\delta}$ with $x = 0.0, 0.06, 0.10, 0.14, 0.15, 0.17$, and 0.20 , were prepared by solid-state re-

action from high-purity Nd_2O_3 , CeO_2 , and CuO . Stoichiometric mixtures of the starting materials were ground thoroughly and heated in air using an Al_2O_3 crucible at 950°C for 12 h. The resulting powders were re-ground and pressed into pellets at 1 kbar and fired in air at 1100°C for 12 h, followed by quenching to room temperature. Both magnetization and resistivity measurements indicated that all of the samples quenched in air are not superconducting above 2 K. In order to obtain superconductivity, it was necessary to anneal the sintered pellets in a reducing atmosphere. We placed these pellets in a furnace chamber with an Al_2O_3 boat filled with fresh titanium sponge next to the sample. This sample chamber was pumped by a diffusion pump to a pressure near 10^{-5} Torr. The samples were then annealed under a vacuum at 875°C for 6 h, maintaining the pressure at 10^{-5} torr. Finally, the samples were furnace cooled to room temperature in 2 h.

X-ray diffraction measurements indicated that both the air quenched and vacuum annealed samples are phase pure for $x \leq 0.20$. All of the diffraction peaks and peak intensities were indexed and matched by a tetragonal Nd_2CuO_4 -type structure with crystal symmetry $I4/mmm$. These lattice parameters determined using an internal silicon standard ($a = 0.543083$ nm) are tabulated in Table I.

Meissner effect, diamagnetic shielding, and normal-state magnetic-susceptibility measurements were obtained between 5 and 300 K using a commercial⁸ superconducting quantum interference device (SQUID) magnetometer. Meissner effect and shielding measurements were obtained in applied fields ranging from 10 to 100 Oe. For the two bulk superconducting samples (see the discussion in the following), the amplitude of the diamagnetic signal yields a Meissner fraction of 30%. No corrections were made for demagnetizing effects. The

TABLE I. Lattice parameters for the $\text{Nd}_{2-x}\text{Ce}_x\text{CuO}_{4-\delta}$ air-quenched (upper part) and vacuum-annealed (lower part) samples.

x	a (nm)	c (nm)	V (nm^3)
0.00	0.3930	1.213	0.1873
0.06	0.3943	1.214	0.1887
0.10	0.3951	1.212	0.1893
0.14	0.3949	1.209	0.1886
0.15	0.3951	1.210	0.1890
0.17	0.3953	1.209	0.1889
0.20	0.3948	1.206	0.1880
0.06	0.3942	1.213	0.1886
0.14	0.3948	1.210	0.1886
0.15	0.3959	1.211	0.1899
0.17	0.3946	1.207	0.1880
0.20	0.3946	1.205	0.1876

size of this Meissner effect is considerably larger than normally obtained for polycrystalline superconducting specimens in this system and confirms the bulk nature of superconductivity in these two samples.

The dc electric resistivity $\rho(T)$ measurements were performed on rectangular specimens cut from sintered pellets employing a standard dc four-probe technique. To ensure good contacts between the electrical leads and the sample, four platinum wires were attached by silver epoxy on the sample surface, followed by annealing at 400°C in air for the air quenched samples and in a N_2 atmosphere for the vacuum annealed samples for $\frac{1}{2}$ h to help the silver diffuse easily around the contacts on the sample surface. This process reduced the contact resistance dramatically.

RESULTS AND DISCUSSION

Previous researchers^{1,9} have noted the strong correlation of the superconductor-nonsuperconductor phase change with the temperature dependence of the resistivity for $\text{Nd}_{2-x}\text{Ce}_x\text{CuO}_{4-\delta}$ prepared in a reducing atmosphere. For $x \leq 0.14$, the temperature dependence of the resistivity behaves like a semiconductor ($d\rho/dT < 0$), although the resistivity steadily decreases with increasing x . The onset of bulk superconductivity is observed abruptly at $x=0.14$. When x exceeds 0.18, superconductivity disappears and the resistivity exhibits a typical metallic behavior. Beyond this concentration, the resistivity still decreases with increasing x and the slope $d\rho/dT$ becomes positive. These results are basically consistent with our present studies. Because of these properties, Liang *et al.*¹⁰ assumed the optimum superconducting composition to lie very close to the crossover from semiconductor to metallic-type conductivity. However, we feel that these resistivity data are poorly understood by a simple model of a semiconductor-metal transition.^{1,10} From our detailed studies, we find no evidence for a semiconductor-metal transition near the superconducting-nonsuperconducting boundary in the vacuum-

annealed or air-quenched samples as a function of Ce content.

In Fig. 1(a) we show the resistivity data of the air-quenched samples in the temperature range 2–400 K for $x=0.06, 0.14, 0.15, 0.17,$ and 0.20 . The $\rho(T)$ increases monotonically with decreasing temperature. All of these resistivity curves can be fitted above 55 K by the equation

$$\rho(T) = \alpha \ln(T) + \beta T + \gamma. \quad (1)$$

Other functional forms such as A/T^n or $Ae^{-b/T}$ do not fit the data.

After annealing at 875°C in a vacuum, the samples with compositions $x=0.15$ and 0.17 showed bulk superconductivity with $T_c=26$ K, and the materials with compositions $x=0.06, 0.10, 0.14,$ and 0.20 displayed traces of superconductivity with the same T_c . The resistivity data on the samples annealed under vacuum with $x=0.06, 0.10, 0.14, 0.17,$ and 0.20 are shown in Fig. 1(b) in the temperature range 2–400 K. For $x < 0.17$, each resistivity curve above 55 K can also be fitted by Eq. (1).

We note that the anomalous behavior of the temperature dependence of the electrical resistivity described by Eq. (1) is normally associated with the Kondo effect.¹¹ The explanation of the Kondo effect is based on the exchange interaction between the spins of the conduction electrons and the localized magnetic moments in the lat-

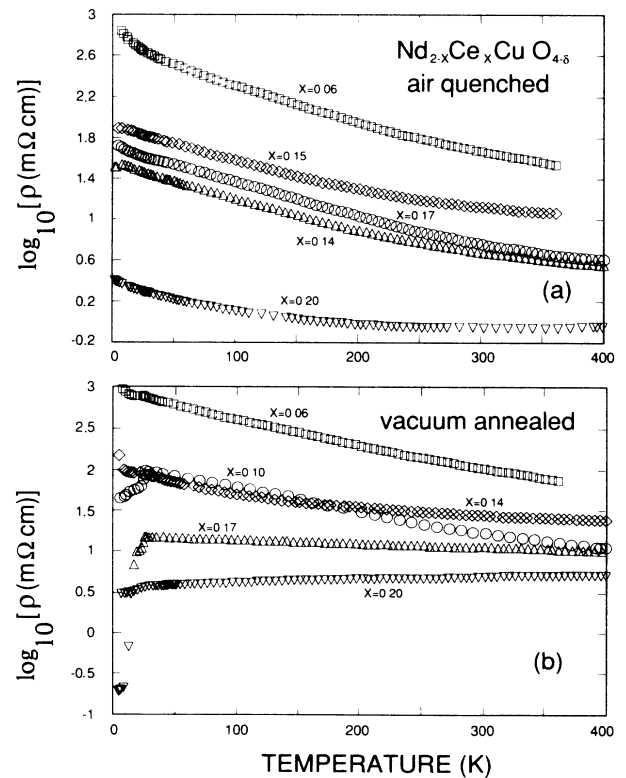


FIG. 1. The logarithm of the dc electrical resistivity as a function of temperature for the air-quenched samples (a) and the vacuum-annealed samples (b).

tice. With a negative exchange constant this interaction in second-order perturbation theory leads to an increase of localized-spin disorder resistivity with decreasing temperature. The minimum in the $\rho(T)$ curve then results from the combined effect of this type of spin-disorder scattering and phonon scattering.

In the $\text{Nd}_{2-x}\text{Ce}_x\text{CuO}_{4-\delta}$ materials, the high-temperature ($55 < T < 400$ K) magnetic-susceptibility measurements indicated that the magnetic moments come from Nd^{3+} ions, while the Ce ions are close to $4+$, with negligible moments. Due to the highly localized character of the rare-earth $4f$ electrons, direct magnetic coupling between the localized Nd^{3+} moments is negligibly small. Therefore, in the absence of a strong indirect coupling, it is conceivable that the rare-earth metallic system $\text{Nd}_{2-x}\text{Ce}_x\text{CuO}_{4-\delta}$ shows a Kondo anomaly in the nondilute case. Here the Ce is introduced to donate electron carriers in the Cu-O planes, which are necessary for both the Kondo effect and the superconductivity to appear, since Nd_2CuO_4 is an insulator as determined by the resistivity measurement.

Kondo^{11,12} derived an expression for the spin-disorder resistivity based on the assumption that a local moment exists, and the effective s - f exchange interactions between the conduction electrons and a single local moment can be written as

$$\mathcal{H} = -\Gamma |g - 1| \mathbf{s} \cdot \mathbf{J}, \quad (2)$$

where Γ is an exchange parameter measuring the strength of the interaction, g is the Landé g factor, \mathbf{s} is the spin operator of the conduction electrons at the local moment site, and \mathbf{J} is the spin associated with the local moment.

Kondo's expression for spin-disorder resistivity then reads

$$\rho_K = \rho_s \left[1 + 2N(E_F)\Gamma |g - 1| \ln \left(\frac{T}{T_F} \right) \right], \quad (3)$$

where ρ_s denotes normal spin-disorder resistivity, T_F the Fermi temperature, and $N(E_F)$ the density of states at the Fermi energy. The total resistivity is then the sum of ρ_K and the contribution from the phonon scattering, which shows a linear dependence over a wide temperature range. By comparing Eqs. (1) and (3), we have

$$\gamma = \rho_s - 2\rho_s N(E_F)\Gamma |g - 1| \ln T_F, \quad (4)$$

$$\alpha = 2\rho_s N(E_F)\Gamma |g - 1|, \quad (5)$$

$$\frac{\gamma}{\alpha} = -\ln T_F + [2N(E_F)\Gamma |g - 1|]^{-1}. \quad (6)$$

When $\Gamma < 0$ (antiferromagnetic coupling), one finds a resistivity minimum at

$$T_{\min} = -\frac{\alpha}{\beta}. \quad (7)$$

The numerical values of α , β , and γ , as well as γ/α and T_{\min} obtained by fitting the resistivity curves using Eq. (1) are listed in Table II for both air-quenched and vacuum-annealed samples. The parameters α , β , and γ

TABLE II. Air-quenched (upper part) and vacuum-annealed (lower part) samples.

x	α	β	γ	γ/α	T_{\min} (K)
0.06	-210.0	0.45	1180	-5.6	466.7
0.10	-30.0	0.045	168	-5.6	666.7
0.14	-15.8	0.032	85.0	-5.4	493.8
0.15	-38.1	0.086	204.7	-5.4	443.0
0.17	-26.0	0.054	138.0	-5.3	481.5
0.20	-0.78	0.0024	4.65	-6.0	325.0
0.06	-405.0	0.720	2195.0	-5.4	562.5
0.10	-67.4	0.134	360.4	-5.4	502.7
0.14	-32.2	0.053	194.3	-6.0	607.5
0.15	-23.4	0.017	155.7	-6.7	1377.4

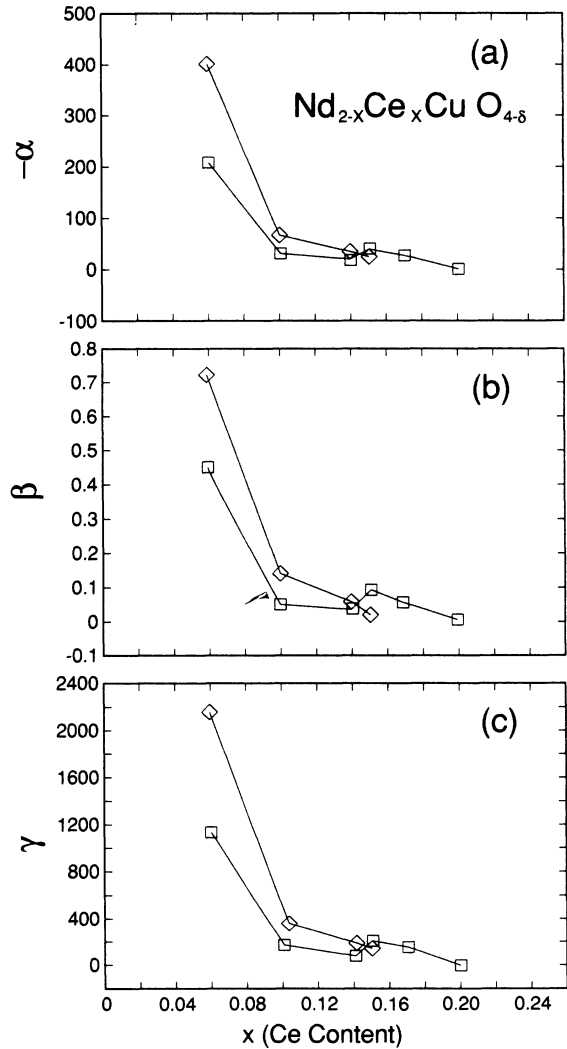


FIG. 2. The least-squares fitting parameters vs the Ce content for air-quenched (\square) and vacuum-annealed (\diamond) samples. See Eq. (1) and the explanation of these parameters in the text.

are plotted versus the Ce composition in Fig. 2. The magnitude of α is a measure of the magnetic scattering strength. The negative values of α reflect a negative Γ indicating an antiferromagnetic coupling between conduction electrons and the localized Nd^{3+} moment. On the other hand, the magnitude of β is a measure of the phonon scattering. For the vacuum-annealed samples, α , β , and γ decrease quickly as the Ce composition increases. However, for the air-quenched samples, α , β , and γ initially decrease with increasing Ce composition, but start to increase slightly when x exceeds 0.14. In these plots of air-quenched samples, each plot has a peak centered at $x=0.15$ between the composition range of $x=0.14-0.17$. We note that this peak disappears when the samples are annealed in vacuum, and bulk superconductivity is observed in the composition range of $x=0.14-0.17$. Although the values of α , β , and γ change by two to three orders of magnitude across the series, the values of γ/α only vary from -6.7 to -5.1 , with a mean value of around -5.5 . The large changes of α and γ with increasing Ce composition imply that the normal spin-disorder resistivity ρ_s is very sensitive to the Ce doping. In Fig. 3 the ratio γ/α is plotted versus x . The values of γ/α for vacuum-annealed samples initially stay constant as x increases. When x exceeds 0.1, the γ/α values become more negative, and drop to -6.7 at $x=0.15$. For the air-quenched samples, the values of γ/α are approximately constant for $x \leq 0.17$. The γ/α value drops to -6.0 at $x=0.2$. As implied by Eq. (6), the quantity γ/α depends on T_F , $N(E_F)$, and Γ , where Γ is a negative con-

stant in this case. Therefore, the change of γ/α is possibly caused by two factors: the shift of Fermi energy by doping Ce into the lattice and the change of the density of states at the Fermi level.

We note that the two curves in Fig. 3 are similar in shape, just shifted by approximately $\Delta x=0.07$. This observation can be explained in terms of the roles played by the Ce doping and oxygen deficiency. The effect of increasing oxygen deficiency (δ) can be compensated by reducing the Ce content (x).

The last quantity listed in Table II is the T_{\min} obtained by using Eq. (7), which does not change monotonically with increasing Ce composition. The value of T_{\min} varies from 325 to 1377 K depending on x . The resistivity minimum around 325 K is actually observed for the air quenched sample at $x=0.20$ as shown in Fig. 1. In order to see the resistivity minima for other samples, we would need to go to higher temperatures. However, we do not expect to see the resistivity minimum at 1377 K, as the sample will decompose before reaching this temperature.

As an example of the resistivity curve fit, Fig. 4 shows the temperature dependence of resistivity with solid lines representing the least-squares fit. Above 55 K all the solid lines going through each data point represent the quality of these fits. At about 55 K, the actual resistivity data begin to deviate from these solid lines as temperature decreases. Such deviation can be attributed to the effect of the crystalline electric field. Magnetization measurements in the temperature range 2–400 K indicate that all $\text{Nd}_{2-x}\text{Ce}_x\text{CuO}_{4-\delta}$ materials exhibit susceptibili-

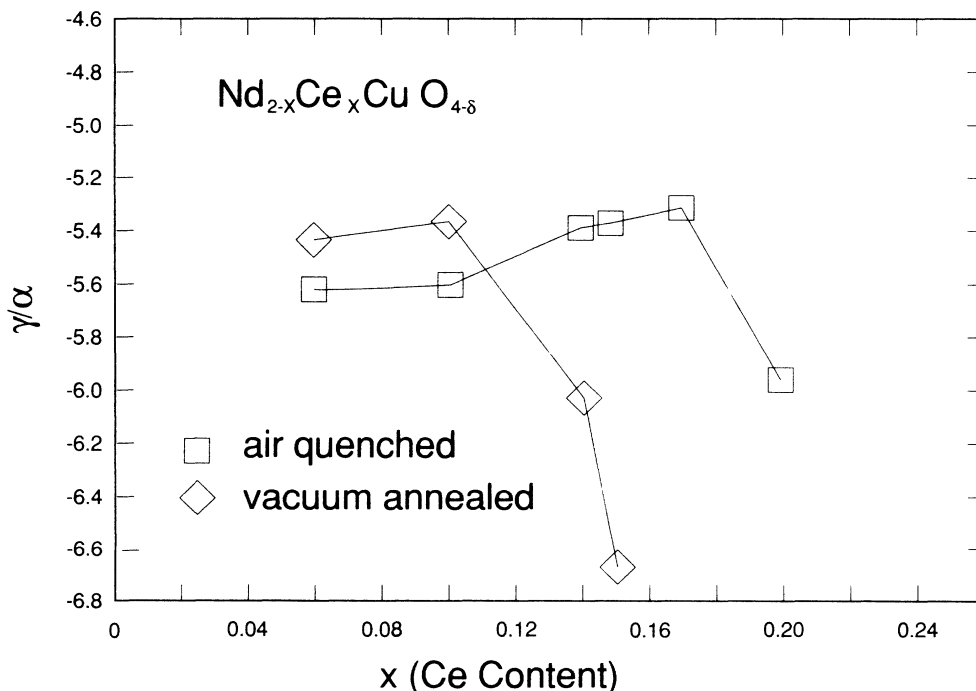


FIG. 3. The ratio of γ/α (see the text) as obtained by the least-squares fit vs the Ce content.

ties typical of Nd^{3+} with a crystalline electric field moment reduction below 55 K. This is demonstrated in Fig. 5, where the inverse susceptibility is plotted versus temperature for the air-quenched sample with $x=0.14$.

For the vacuum-annealed samples with $x > 0.17$, the logarithmic temperature term in the resistivity disappears, and the slope of the resistivity curves becomes positive. Although the materials still display traces of superconductivity, bulk superconductivity is observed only in the composition range $0.14 < x \leq 0.17$, where contributions to the resistivity from both the magnetic scattering and phonon scattering exist. We conclude that when x is less than 0.14, the magnetic interactions are too strong for superconductivity to appear. On the other hand, when x exceeds 0.17, the total disappearance of magnetic

scattering is also detrimental to the superconducting state. These resistivity data show that in addition to the magnetic scattering contribution, a significant phonon term indicative of metallic behavior exists throughout the entire range. Therefore, a model that relies on a sharp metal-insulator transition is not appropriate for this system.

Recent resistivity measurements on superconducting $\text{Nd}_{2-x}\text{Ce}_x\text{CuO}_{4-\delta}$ single crystals¹³ indicate that the resistivity curve in the ab plane above T_c has positive slope [$d\rho(T)/dT > 0$]. However, this temperature dependence is not linear in the entire temperature range studied (T_c to 300 K). A possible fit for these single-crystal resistivity data may need a combination of a metallic term and a term due to magnetic scattering. Although the metallic term dominates in this case, one can not rule out the possibility of a large contribution from the magnetic scattering perpendicular to the ab plane, which has not been measured for the single crystal.

Thus the main question of whether the negative slope [$d\rho(T)/dT < 0$] above T_c is an intrinsic property along one, or more, principal crystallographic axes of these compounds remains open. The component of the resistivity that can be associated with the Kondo effect may be dominated by interactions perpendicular to the ab plane.

In addition to the anisotropy considerations, we note that the normal-state resistivity data remain very sensitive to the Ce concentration. To make a comparison of the single-crystal resistivity data with our ceramic samples, a knowledge of the absolute accuracy of the Ce content in the single crystals is necessary. For the vacuum-annealed samples with $x > 0.17$ we also observe the normal-state resistivity data with $d\rho(T)/dT > 0$. Therefore, our resistivity data of ceramic $\text{Nd}_{2-x}\text{Ce}_x\text{CuO}_{4-\delta}$ do not contradict these single-crystal results.

To test our polycrystalline results, we prepared plate-like (3mm) $\text{Nd}_{2-x}\text{Ce}_x\text{CuO}_{4-\delta}$ single crystals,¹⁴ which were annealed in air only, and therefore were not superconducting. Our resistivity measurements in the ab plane in the temperature range 2–400 K are consistent with the polycrystalline results discussed in this paper, that is $d\rho(T)/dT < 0$. While, it is still necessary to perform single-crystal studies on several samples with varying cerium and oxygen concentrations to conclusively demonstrate the absence of intergranular effects in polycrystalline data, our one single-crystal measurement to date¹⁴ indicates that our polycrystalline resistivity results are intrinsic to these materials.

The experimental density of our ceramic samples is approximately 90% of the theoretical value of 7.25 g/cm^3 . This is a rather high value considering the powder synthesis methods employed. This high density is of great importance in determining the intrinsic properties of the materials. As another comparison of our ceramic compounds with the single crystals, we note that our vacuum-annealed ceramic sample with $x=0.20$ has a resistivity value at 300 K of $0.9 \text{ m}\Omega \text{ cm}$, which is comparable to the single crystal resistivity¹³ at 300 K for $x=0.16$. Therefore, we conclude that the intergrain contribution to the resistivity for these ceramic samples stud-

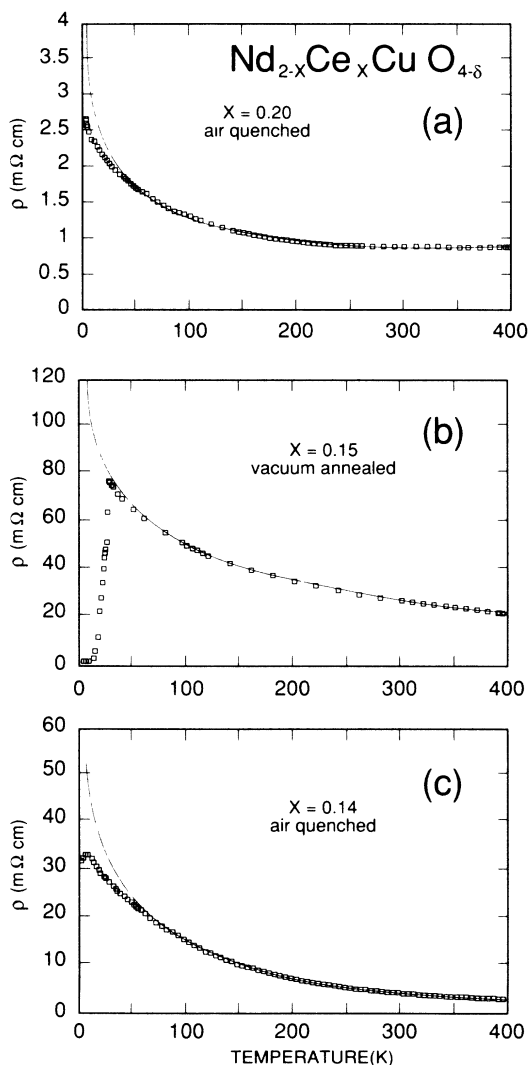


FIG. 4. Temperature dependence of resistivity for (a) $x=0.20$, air quenched; (b) $x=0.15$, vacuum annealed; (c) $x=0.14$, air quenched. The solid lines represent the least-square fits (see Table II).

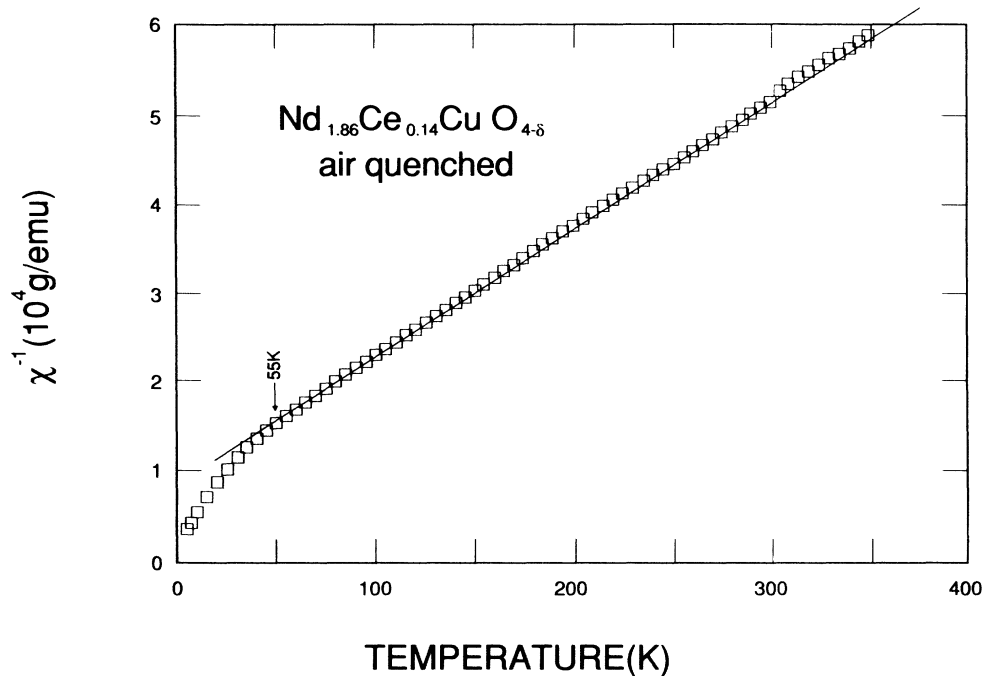


FIG. 5. The inverse magnetic susceptibility as a function of temperature for an air-quenched sample with $x=0.14$ taken in an applied field of 2.0 kOe.

ied in this work must be negligibly small, and does not affect significantly the determination of the intrinsic properties.

In summary, we have prepared single-phase high-density $\text{Nd}_{2-x}\text{Ce}_x\text{CuO}_{4-\delta}$ materials. The Kondo effect is offered as a plausible, quantitative explanation of the resistivity data for both air-quenched and vacuum-annealed samples. Bulk superconductivity is observed only in the narrow range of Ce composition. The linear phonon contribution to the resistivity exists across the entire Ce composition ($x > 0$) indicating that the oc-

currence of bulk superconductivity is not simply due to a semiconductor-metal transition.

ACKNOWLEDGMENTS

The authors wish to thank Huixia Shu for assisting with the nonlinear-least-squares curve fitting. We are also grateful to P. Klavins for technical assistance. Research at Davis and Livermore performed under the auspices of the U.S. Department of Energy for Lawrence Livermore National Laboratory under Contract No. W-7405-ENG-48.

- ¹Y. Tokura, H. Takagi, and S. Uchida, *Nature* **337**, 345 (1989).
- ²J. T. Markert, and M. B. Maple, *Solid State Commun.* **70**, 145 (1989).
- ³J. T. Markert, E. A. Early, T. Bjornholm, S. Ghamaty, B. N. Lee, J. J. Neumeier, R. D. Price, C. L. Seaman, and M. B. Maple, *Physica* **158C**, 178 (1989).
- ⁴H. Müller-Buschbaum, *Angew. Chem. Inst. Engl.* **16**, 674 (1977).
- ⁵V. H. Müller-Buschbaum and W. Wollschläger, *Z. Anorg. Allg. Chem.* **414**, 76 (1975).
- ⁶H. Takagi, S. Uchida, and Y. Tokura, *Phys. Rev. Lett.* **62**, 1197 (1989).
- ⁷P. Hahn, H. B. Radousky, J. L. Peng, and R. N. Shelton (unpublished).
- ⁸Acquired from Quantum Design, Inc., San Diego, CA.

- ⁹J. L. Peng, R. N. Shelton, and H. B. Radousky, *Solid State Commun.* **71**, 479 (1989).
- ¹⁰G. Liang, J. Chen, M. Croft, K. V. Ramanajachary, M. Greenblatt, and M. Hegde, *Phys. Rev. B* **40**, 2646 (1989).
- ¹¹J. Kondo, *Prog. Theor. Phys.* **41**, 1199 (1964).
- ¹²J. Kondo, *Solid State Physics*, edited by F. Seitz, D. Turnbull, and H. Ehrenreich (Academic, New York, 1969), Vol. 23, p. 183.
- ¹³J. M. Tarascon, E. Wang, L. H. Greene, B. G. Bagley, G. W. Hull, S. M. D'Egidio, P. F. Miceli, Z. Z. Wang, T. W. Jing, J. Clayhold, D. Brawner, and N. P. Ong, *Phys. Rev. B* **40**, 4494 (1989).
- ¹⁴J. L. Peng, L. Zhang, P. Klavins, J. Z. Liu, R. N. Shelton, and H. B. Radousky (unpublished).